Modeling and Analysis of a Switched Reluctance Motor Drive System

Mikho R. Mikhov[1]

Abstract – **The behavior of a switched reluctance motor drive system with speed control has been analyzed in this paper. The investigations in the respective dynamic and static regimes have been carried out through modeling and computer simulation. The developed models and the results obtained can be used as illustration in the process of teaching about such types of drive systems.**

Keywords – **Electric drive systems, Switched reluctance motor drives.**

I. INTRODUCTION

Switched reluctance motors (SRMs) have some features that make them an attractive alternative to existing DC and AC motors in adjustable speed drives. The SRM's main advantages can be summarized as follows [1], [2], [3]:

- simple and robust structure;
- each phase winding is independent and this makes the machine highly reliable;
- low power losses and high efficiency;
- high power-mass ratio;
- good heat dissipation characteristics;
- high torque-to-inertia ratio and good dynamics;
- motor torque is independent of the phase current polarity, thus the respective converter usually requires only one switch per phase;
- high speed capabilities.

In recent years SRM drive systems have been used in many applications such as electric vehicles, robotics, textiles, aerospace, office automation, machine tools, and many more [3].

II. SPECIFIC FEATURES OF SRM DRIVES

SRMs are doubly salient, singly excited electrical machines with passive (windingless) rotors. The motor phases are turned on sequentially through DC voltage pulses, which result in unipolar controlled current. Motion is produced because of the variable reluctance in the air gap between the stator and the rotor. When a stator winding is energized, producing a single magnetic field, reluctance torque is produced by the tendency of the rotor to move to its minimum reluctance position [1].

The cross-section of the SRM under consideration is shown in Fig. 1. The motor is made of laminated stator and rotor cores with 6 poles on the stator and 4 poles on the rotor. The phase number is $m = 3$ and each phase has concentrated coils placed on one pair of stator poles.

[1]Mikho R. Mikhov is with the Faculty of Automatics, Technical University of Sofia, 8 Kliment Ohridski Str., 1797 Sofia, Bulgaria, E-mail: mikhov@tu-sofia.bg

The magnetic circuit symmetry leads to almost zero mutual flux linkage in the SRM phases even under saturated conditions. This means that the motor may work with $m-1$ phases since no induced voltage or current will appear in the short-circuited phase.

The phase self-inductance L_i varies with the rotor position, and in presence of saturation the respective dependence is nonlinear (Fig. 2).

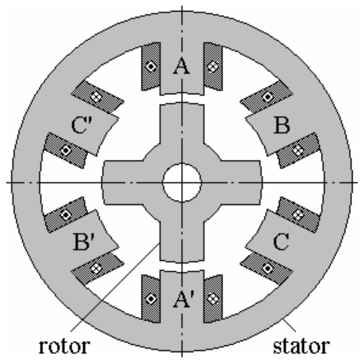

Fig. 1. Cross-section of a 6/4 switched reluctance motor.

The magnetic saturation influence is evident from Fig. 3, where a flux curve family is shown.

The motoring and regenerative regimes are illustrated with the simplified diagrams shown in Fig. 3. Positive (motoring) torque is produced when the inductance is rising as the shaft angle is increasing. A negative (breaking) torque is produced by supplying the motor winding with current while the inductance is decreasing.

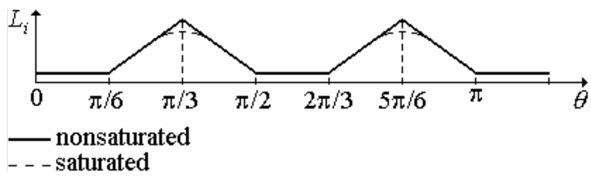

Fig. 2. The self-inductance profile for one motor phase.

The average torque T_i can be controlled by adjusting the winding current magnitude I_i or by varying the dwell angle θ_d . To reduce the torque ripples, it is advisable to keep the dwell angle constant and change the current magnitude.

The communication sequences are shown in Fig. 4.

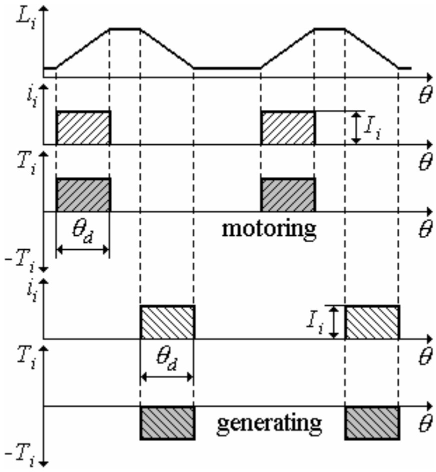

Fig. 3. Diagrams illustrating the operation modes of the motor.

The main problems of SRM drive practical implementation are as follows:

- the SRMs must always be electronically commutated and thus cannot run directly from a DC bus or an AC line;
- their salient structure causes strong non-linear magnetic characteristics, complicating its analysis and control;
- the pulsed nature of torque production leads to torque ripple and noisy effects.

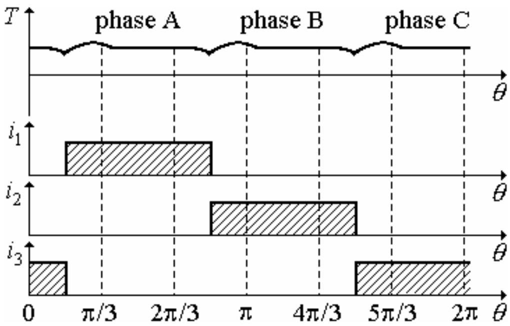

Fig. 4. Commutation sequences.

The major disadvantage of having a high torque ripple can be overcome by using suitable control methodologies [2], [10].

III. Modeling of the SRM Drive System

A simplified block diagram of the drive system under consideration is shown in Fig.5. The corresponding notations are as follows: SC - speed controller; RC - reference current block; CC - current controllers block; CB - converter control block; PC – power converter; PS - position sensor; SF - speed feedback block; CF – current feedback block; L - load of the electric drive; V_{sr} - speed reference signal; V_{cr} - three-phase current reference signals for the phases *a*, *b* and *c* respectively; $2\Delta i$ - reference hysteresis band; V_{sf} - speed feedback signal; V_{cf} - current feedback signals; V_d - DC link voltage; C - filter capacitor; ω - angular motor speed; θ - angular position; T_l - load torque applied to the motor shaft.

The electric equations used to represent the *m*-phase SRM are as follows [2], [3], [4]:

$$\left.\begin{aligned} v_1 &= R_s i_1 + \frac{d\Phi_1(\theta, i_1)}{dt}; \\ &\ldots \\ v_i &= R_s i_i + \frac{d\Phi_i(\theta, i_i)}{dt}; \\ &\ldots \\ v_m &= R_s i_m + \frac{d\Phi_m(\theta, i_m)}{dt}, \end{aligned}\right| \tag{1}$$

where:

$v_{i(i=1\div m)}$ is the voltage applied across the respective stator winding;

i_i - the phase current;

R_s the stator phase resistance;

$\Phi_i(\theta, i_i)$ - the phase flux linkages for a given rotor position θ and excitation current i_i.

The motion equations are as follows:

$$J\frac{d\omega}{dt} = T + T_l; \tag{2}$$

$$\frac{d\theta}{dt} = \omega, \tag{3}$$

where:

J is the total inertia referred to the motor shaft;

T - the motor torque.

The total instantaneous torque is given by:

$$T = \sum_{i=1}^{m} T_i, \tag{4}$$

where the respective component is:

$$T_i = \frac{\partial}{\partial\theta}\int_0^{i_i} \Phi_i(\theta, i_i)\,di_i. \tag{5}$$

The equation for each phase can be expressed as follows:

$$\begin{aligned} v_i &= R_s i_i + \frac{\partial\Phi_i(\theta, i_i)}{\partial i_i}\frac{di_i}{dt} + \frac{\partial\Phi_i(\theta, i_i)}{\partial\theta}\frac{d\theta}{dt} = \\ &= R_s i_i + L_i(\theta, i_i)\frac{di_i}{dt} + E_i(\omega, \theta, i_i), \end{aligned} \tag{6}$$

where:

$L_i(\theta, i_i) = \dfrac{\partial\Phi_i(\theta, i_i)}{\partial i_i}$ is the instantaneous inductance;

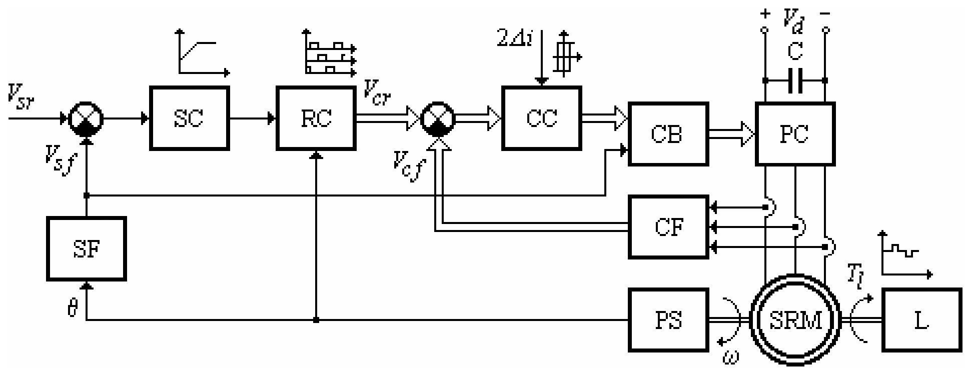

Fig. 5. Block diagram of the drive system under consideration

$E_i(\omega,\theta,i_i) = \dfrac{\partial \Phi_i(\theta,i_i)}{\partial \theta}\omega$ - the instantaneous back EMF.

The SRM mathematical model is highly nonlinear due to the magnetic saturation influence on the $\Phi_i(\theta,i_i)$ curve family (Fig. 6). Only in the absence of saturation, the instantaneous torque is:

$$T = \sum_{i=1}^{m} \frac{1}{2} i_i^2 \frac{\partial \Phi_i(\theta,i_i)}{\partial \theta}. \qquad (7)$$

There are several possible strategies to energize a SRM. For this study hysteresis current control has been chosen. The respective phase current controllers have a programmable hysteresis band $2\Delta i$, which determines the modulation frequency of the power converter. The principle of current chopping is shown in Fig. 7, where i_{ir} is the respective reference phase current waveform.

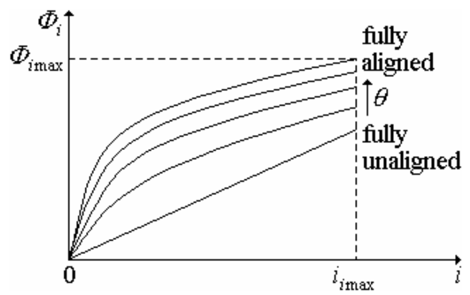

Fig. 6. Flux/current curves.

The current i_i cannot instantaneously rise or fall in the respective phase circuit. For that reason, the voltage to the stator winding is applied in advance by θ_a and the current turn-off is initiated in advance by θ_b. To optimize the drive system efficiency, it is necessary to choose appropriate values for θ_a and θ_b.

The following torque/speed zones can be distinguished (Fig.8):

1. $T = \text{const} \quad (0 < \omega \le \omega_1)$;
2. $T\omega = \text{const} \quad (\omega_1 < \omega \le \omega_2)$;
3. $T\omega^2 = \text{const} \quad (\omega_2 < \omega \le \omega_{\max})$.

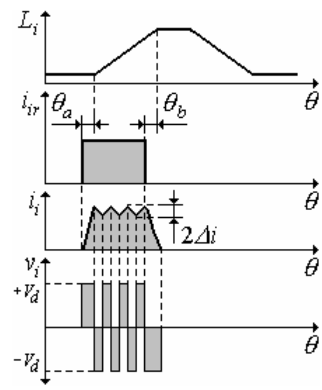

Fig. 7. Operational waveforms of the DC supply converter.

The angles θ_a and θ_b values should be corrected in compliance with both speed and operation modes.

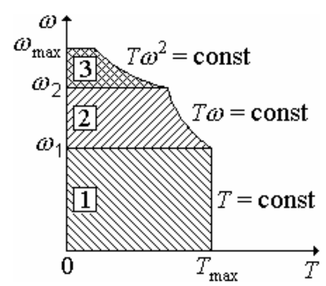

Fig. 8. Torque/speed zones of the SRM drive.

Using the MATLAB/SIMULINK software package some computer simulation models of electric drives with SRM have been developed. Detailed study of the drive system under consideration has been carried out for the dynamic and static regimes at various loading, disturbances and work conditions.

IV. Some Simulation Results

The current forming for one motor phase is illustrated in Fig. 9, where are represented the respective current and voltage waveforms.

Fig. 10 shows the phase current waveforms i_1, i_2, and i_3 obtained for reference current level $i_{ir} = 10\,\mathrm{A}$. The load

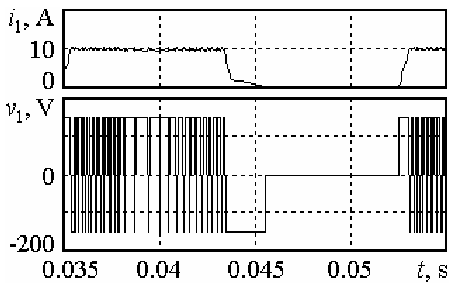

Fig. 9. Current and voltage waveforms for one motor phase.

torque applied to the motor shaft is $T_l = 8\,\mathrm{Nm}$.

Fig. 11 shows current waveforms obtained in steady state regime at low and high motor speeds. In this case the load torque is $T_l = 6\,\mathrm{Nm}$.

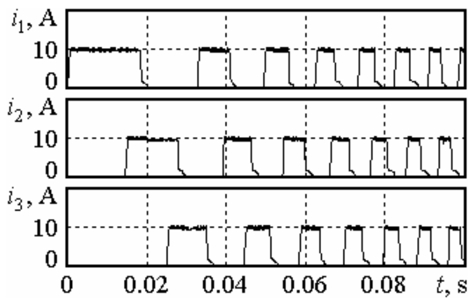

Fig. 10. Three-phase current waveforms.

The starting process and the motor speed stabilization is illustrated in Fig. 12, where the drive system reaction to dis-

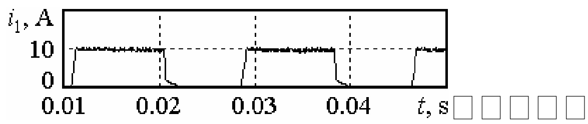

a) at low motor speed

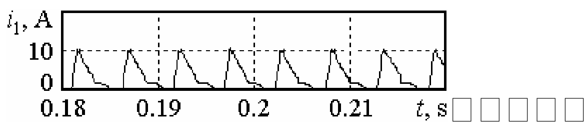

b) at high motor speed

Fig. 11. Current waveforms obtained for various motor speeds.

turbances is represented. The reference speed is $\omega_r = 314$ rad/s and the load changes applied sequentially to the shaft are $\pm\Delta T_l = \pm 0.25 T_l$. As evident, using a suitable speed controller, the drive static error is eliminated.

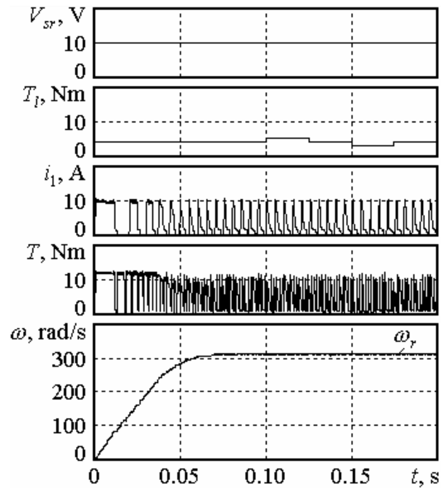

Fig. 12. Starting and motor speed stabilization.

V. CONCLUSION

The performance of a 6/4 three-phase SRM drive system with speed control is analyzed in this paper.

The investigations have been carried out through modeling and computer simulation for the respective transient and steady state regimes of operation.

The developed simulation models and the results obtained can be used for appropriately illustration in the process of teaching about such types of electric drive systems.

REFERENCES

[1] T. J. E. Miller, *Switched reluctance motors and their control*, Oxford, Clarendon Press, 1993.

[2] T. J. E. Miller, Electronic control of switched reluctance machines, Oxford, "Newnes", 2001.

[3] R. Krishnan, *Switched reluctance motor drives*, Boca Raton, CRC Press, 2001.

[4] I. Boldea, S. A. Nasar, *Electric drives*, Boca Raton, CRC Press, 1999.

[5] A. Brosse, G. Henneberger, „Different models of the SRM in state space format for the sensorless control using a Kalman filter", *Power Electronics and Variable Speed Drives, Conference Proceedings,* pp. 269-274, London, UK, 1998.

[6] G. S. Buja, "Control characteristics of the SRM drives, Part II: Operation in the saturated region", *IEEE Transactions on Industrial Electronics,* vol. 41, no. 3, pp. 316-325, 1994.

[7] K. R. Tthompson, P. P. Acarnley, C. French, "Rotor position estimation in a switched reluctance drive using recursive least squares", *IEEE Transactions on Industrial Electronics,* vol. 47, no. 2, pp. 368-379, 2000.

[8] M. R. Mikhov, A. M. Avramov, R. N. Ognyanov, "Perspectives for implementation of switched reluctance motor drives". *Announcements of Union of Scientists*, vol. 3, pp. 160-162, Sliven, 2001.

[9] S. Cao, K. J. Tseng, „A new method for accurate analytical modeling of switched reluctance motor", *International Conference on Power Electronics Drives and Energy Systems for Industrial Growth*, *Conference Proceedings,* pp. 540-545, Perth, Australia, 1998.

[10] S. Mir, M. E. Elbuluk, I. Husain, Torque-ripple minimization in switched reluctance motors using adaptive fuzzy control, *IEEE Transactions on Industry Applications,* vol. 35, no. 2, pp. 461-468, 1999.